Comparison of CRISPR-Cas9 tools for transcriptional repression and gene disruption in the BEVS

Mark Bruder[1], Sadru-Dean Walji[1], and Marc Aucoin[1]

[1]University of Waterloo

May 18, 2021

Abstract

The baculovirus expression vector system (BEVS) is a robust and customizable platform for producing recombinant proteins for basic research and biomedical applications. However, genome instability is an intrinsic property of BEVs, and expression of several viral proteins negatively impacts recombinant protein quantity and quality. The CRISPR-Cas9 system is a powerful tool that simplifies sequence-specific genome editing and effective transcriptional regulation of genes for which disruption may not be appropriate. Here, the effectiveness of the CRISPR-Cas9 system for gene disruption and transcriptional repression in the BEVS was compared. A cell line constitutively expressing the cas9 or dcas9 gene was developed, and recombinant baculoviruses delivering the sgRNA were evaluated for disruption or repression of a reporter gfp gene. Finally, endogenous AcMNPV genes were targeted for disruption or downregulation to affect gene expression and baculovirus replication. This development lays a foundation for optimization of the BEV for improved genome stability and recombinant protein production.

Introduction

The BEVS has many features that make it attractive as a platform for production of recombinant proteins and therapeutics: recombinant*Autographa californica* multiple nucleopolyhedrovirus (AcMNPV) baculovirus expression vectors (rBEVs) are easy to manipulate and have the capacity to carry large DNA inserts; they can be rapidly produced and purified at high titers; they offer scalable and transient expression of target protein(s) without adding significant cost as scale increases; multiple endogenous baculovirus promoters are considered to be among the strongest promoters found in nature and can lead to exceptionally high levels of target gene mRNA; and since there are very few adventitious agents that can propagate in both insect and mammalian cells, the BEVS is generally considered safe. Further, AcMNPV can transduce an incredibly wide variety of cells with low cytotoxicity, including many vertebrate cell lines, primary cells, progenitor, and stem cells, but cannot replicate within these heterologous hosts, making it a potential platform for therapeutic gene delivery . To realize its full potential, however, intrinsic limitations of the BEVS must be addressed: the lytic infection cycle and resulting short bioprocess duration can limit overall yield of the recombinant protein, and large amounts of progeny virus, cellular proteins, and debris from lysed cells are contaminants that necessitate extensive purification steps to achieve product purity . Additionally, instability of the AcMNPV genome leads to the spontaneous loss of large DNA fragments from its genome, which often includes the inserted foreign gene .

The AcMNPV genome is comprised of more than 150 putative open reading frames (ORFs), and despite its complete DNA sequence being reported more than 25 years ago, the majority of ORFs have no proven function . Several genes are required for DNA replication, viral gene expression, and subsequent progeny virus production. However, baculoviruses have a complex biphasic 'life' cycle in which virions are either encapsulated in proteinaceous protective shells named occlusion-derived virions (ODVs) or released from cells as budded virions (BVs). Many genes associated with the ODV phenotype are dispensable for propagation in vitro in cell culture . Typically, evaluating the function of AcMNPV genes involves deletion of the target ORF

from the AcMNPV genome and development of a *trans* -complementing cell line for expression of the deleted gene to enable production of infective virions . Developing deletion-mutant rBEVs and complementing cell lines, however, can be cumbersome, tedious, and time consuming. Gene silencing via RNA interference (RNAi), on the other hand, involves the production of double strand RNA (dsRNA) molecules that inhibit gene expression by triggering the degradation of messenger RNA (mRNA) through the RNA-induced silencing complex (RISC). The dsRNA molecules are typically introduced by transfection of small interfering RNA (siRNA) directly or plasmids from which short hairpin RNAs (shRNA) are transcribed . Target sequence selection, however, often requires extensive empirical validation to identify high silencing efficiency targets, and the effectiveness may be limited by low transfection efficiency and relatively high cytotoxicity of the transfection reagent .

The CRISPR-Cas9 system has seen development for precision genome editing and targeted transcriptome engineering in a multitude of biological organisms over the past decade . Genome editing was recently reported in cultured cells from *Spodoptera frugiperda* (Sf9) and *Trichoplusia ni* (High Five), which are the two commonly used hosts for infection and recombinant protein production in the BEVS, and for genome editing in AcMNPV itself . Here, we have extended upon these recent advancements by developing robust and efficient engineering tools based on Cas9 and its nuclease deficient variant dCas9 for targeted gene disruption via Cas9-mediated dsDNA-cleavage resulting in insertion-deletion (indel) mutations (CRISPRd) and transcriptional repression via dCas9-mediated interference of transcript elongation (CRISPRi), respectively. We show that both technologies are capable of scrutinizing the essentiality (i.e. whether the gene is necessary for expression of viral late genes or production of progeny virions) of the targeted gene. We believe these tools will enable more sophisticated strategies aimed at modulating expression of AcMNPV genes to improve BEVS bioprocessing, and as a tool for screening genomic loci to determine function and essentiality of AcMNPV genes, leading to a minimal rBEV genome.

Materials and Methods

Cells

Sf9 cells were maintained in suspension culture in Gibco SF900 III serum free medium (Fisher Scientific, Whitby ON) as described previously . Sf9 cells were transfected as adherent culture in tissue culture treated 6-well plates (VWR, Mississauga ON) with Escort IV transfection reagent (Sigma-Aldrich, Oakville ON) according to manufacturer directions. To derive the transgenic Sf9-Cas9 and Sf9-dCas9 cell lines, parental Sf9 cells were transfected with the plasmid pOpIE2-Cas9-puro or pOpIE2-dCas9-puro, respectively. Approximately 48 hours post transfection (hpt), growth medium was aspirated and replaced with fresh medium containing 5 μg/ml puromycin (Sigma-Aldrich). Selective pressure was maintained for at least 2 weeks, and resistant cells were pooled, adapted back to suspension culture, and maintained under the same growth conditions as the parental cell line, with or without puromycin.

Plasmid Construction

All plasmids used in this study were constructed using NEBuilder HiFi DNA Assembly master mix (New England Biolabs, Whitby ON) according to manufacturer's directions. Primers used for construction of all plasmids and retargeting sgRNAs were purchased from Integrated DNA Technologies (IDT; Coralville, IA) and are listed in Table S1.

To construct plasmid pOpIE2-Cas9-puro, the cas9-T2A-pac region from pAc-sgRNA-Cas9 (Addgene #49330, Cambridge MA) and a fragment containing the *Orgyia pseudotsugata* MNPV immediate-early 2 promoter (OpIE2) and 3' untranslated region (UTR) , origin of replication (ori), and ampicillin resistance gene (ampR) for propagation in *E. coli* were amplified via PCR and the 2 PCR fragments were used in a Gibson assembly reaction. The resulting plasmid placed the cas9-T2A-puro expression cassette under the control of the constitutive OpIE2 promoter. To generate plasmid pOpIE2-dCas9-puro, the dcas9 ORF was amplified from pdCas9::BFP-humanized (Addgene #44247) and used in a Gibson assembly reaction along with a PCR fragment containing the OpIE2 promoter, T2A-puro cassette, and OpIE2 3' UTR to place the dCas9 gene under the constitutive control of the OpIE2 promoter.

For plasmids containing the OpIE2-GFP cassette and SfU6 sgRNA, the {*mAzami-Green* gene (Addgene #54798; herein referred to as*gfp*) encoding a monomeric green-emitting fluorescent protein gene was PCR amplified and placed between the OpIE2 promoter region and 3' UTR. Separately, the *S. frugiperda* U6 (SfU6) small nuclear RNA (snRNA) promoter was synthesized as a gblock (IDT), and PCR amplified along with the single guide RNA (sgRNA) and transcriptional terminator from plasmid pCFD4-U6:1_U6:3tandemgRNAs (Addgene #49411). The OpIE2-GFP fragments were inserted along with the SfU6-sgRNA DNA fragment into pACUW51 to derive plasmid pOpIE2GFP-sgRNA.

To construct p10-GFP and p6.9-GFP-encoding CRISPR plasmids, first the coding region of the *p10* gene, including upstream and downstream sequences to include its endogenous promoter and 3' UTR, was amplified from AcMNPV genomic DNA and inserted into pACUW51. The *p10* ORF was then replaced with the *gfp* gene, and the SfU6-sgRNA fragment was inserted downstream to derive p10GFP-sgRNA. Finally, the p6.9 promoter region was amplified from AcMNPV genomic DNA and inserted in place of the p10 promoter sequence in p10GFP-sgRNA to yield p6.9GFP-sgRNA.

The spacer sequences used to target Cas9 and dCas9 to specific AcMNPV genomic loci were selected using the sgRNA scorer 2.0 software . Briefly, the coding sequence for the target gene was submitted to the sgRNA scorer 2.0 software which generated a list of putative target sites scored according to their predicted activity. For each gene target, 2-4 target sequences were selected based on two criteria: predicted activity and the strand (template or nontemplate) the target sequence resided on. Inverse PCR was used to retarget sgRNA spacer sequences to the target of interest . Two primers were designed to anneal to the cas9 handle of the sgRNA sequence and to the U6 promoter sequence and extend in opposite directions. The desired targeting spacer sequence was appended to these primer sequences, which were used to amplify the entire plasmid as a linear fragment. The spacer sequence served as the homologous sequence required for Gibson assembly to ligate and re-circularize the new plasmid. The spacer sequences used in this study are presented in Table 1.

Virus generation, amplification, and quantification

Plasmids for homologous recombination at the *polyhedrin* locus in the AcMNPV genome were co-transfected with *flash* BACGOLD (Oxford Expression Technologies Ltd., Oxford UK) genomic DNA according to manufacturer's directions. Supernatant from each transfection was harvested 4-5 days post transfection and used to infect early-exponential phase (˜1.5-2x10^6cells/ml) suspension Sf9 cultures at low multiplicity of infection (MOI) to amplify the rBEVs for 3-4 days or until the viable cell density dropped to ˜80%. After 2 sequential rounds of amplification, the rBEV titer was quantified using end-point dilution assay (EPDA). Briefly, Sf9 cells were diluted to ˜2.0x10^5 cells/ml, and 100 µl was used to seed each well of a 96-well plate (VWR). The virus was serially diluted (10^{-2} to 10^{-8}), and 10µl of each dilution was added, in 12 replicates, to the 96-well plate. Plates were incubated for seven days at 27 °C, after which they were checked for green fluorescence using a fluorescence microscope. Results were converted from $TCID_{50}$ and reported as plaque forming units per ml (pfu/ml).

Infections

Sf9-dCas9 , Sf-Cas9, or the parental Sf9 cells were infected with rBEVs at a density of ˜1.5-2x10^6 cells/ml and MOI of 3. Samples were taken at 24, 48, and 72 hours post infection (hpi) and cells were fixed with 2% paraformaldehyde for ˜30 minutes prior to further analysis.

Flow cytometry and analysis

Samples were analyzed using a FACSCalibur flow cytometer (BD Biosciences, San Jose CA) equipped with a 15-mW air-cooled argon-ion laser with an excitation frequency of 488 nm. Samples were run at the low flow setting (12 µl/min) and 10000 events were collected. Analysis of flow cytometry data was performed using FlowJo® V10 flow cytometry analysis software (FlowJo LLC, Ashland, OR). Briefly, after applying gates to remove debris and intrinsic cellular fluorescence from the analysis, median fluorescence intensity in FL1 was calculated.

Semi-quantitative reverse transcription polymerase chain reaction (RT-qPCR)

Infected cells (˜1.5-2x10^6 cells/ml, MOI = 3) were collected at 0, 24, 48, and 72 hpi by centrifugation at 1000 x *g* for 10 min at 4 °C. RNA was extracted using the Geneaid Total RNA Mini kit (FroggaBio, Concord ON) and 500 ng was used as template for first-strand cDNA synthesis using the SensiFAST cDNA synthesis kit (FroggaBio) according to manufacturer's directions. Semi-quantitative PCR was performed using the SensiFAST SYBR Hi-ROX kit (FroggaBio) according to manufacturer's directions on an Applied Biosystems StepOnePlus Real-Time PCR System (Fisher Scientific). Primer pairs used for qPCR are given in Table S1.

Western blot

Infected cells (˜1.5-2x10^6 cells/ml, MOI = 3) were collected at 0, 24, 48, and 72 hpi by centrifugation at 1000 x *g* for 10 min at 4 degC. The cells were lysed in RIPA buffer (Fisher Scientific), quantified by BCA assay (Fisher Scientific), and ˜10 µg of protein was separated by electrophoresis in 10\% TGX Stain-Free precast mini SDS-PAGE gels (Bio-Rad, Mississauga ON) according to manufacturer's directions. After transfer to PVDF membranes, Western blot analysis was performed with anti-Cas9 (MAC133; Sigma-Aldrich) or anti-GP64 (AcV5, Fisher Scientific) as primary antibodies and goat anti-mouse IgG HRP secondary (Bio-Rad) and imaged on a ChemiDoc MP Imager (Bio-Rad). The Image Lab software was used for further image processing (Bio-Rad).

Quantification of baculovirus particles using flow cytometry

Sample preparation for analysis via flow cytometry was described previously . Briefly, samples were diluted in D-PBS and fixed with paraformaldehyde for ˜1 hour, after which the samples were subjected to one freeze-thaw cycle followed by incubation with Triton X-100 to permeabilize the membrane. The nucleic acid stain SYBR Green I was added and incubated at 80 °C for 10 min in the dark to stain double stranded DNA. After cooling on ice, the samples were analyzed via flow cytometry. Flow-Set Fluorospheres (Beckman Coulter, Mississauga ON) were used for calibration and all samples were run in triplicate.

Results

Development of a Sf9 cell line for constitutive expression of Cas9 and dCas9

Expression of the Cas9 and dCas9 proteins was conferred via the development of transgenic Sf9 cell lines constitutively expressing the*cas9* or *dcas9* gene. The plasmids pOpIE2-Cas9-puro and pOpIE2-dCas9-puro include either the *cas9* or *dcas9* gene and the *pac* gene sequences separated by the viral T2A element . In this configuration, the *(d)cas9* and *pac* genes are transcribed and translated as a single mRNA molecule but due to the T2A self-cleaving peptide, (d)Cas9 and PAC, which encodes puromycin*N*- acetyltransferase and confers resistance to the antibiotic puromycin, are produced unfused in a 1:1 ratio.

After selection for stable integration of the plasmid with puromycin for at least 2 weeks, resistant cells were pooled and maintained in suspension culture. Although routine maintenance of these cell lines provided no evidence that ectopic expression of either Cas9 proteins had any effect on their growth, prior to performing any gene disruption or transcriptional repression experiments, the cell lines were characterized with infection experiments to determine whether there were any distinguishable differences between them and parental Sf9 cells. As shown in Figure 1A, transcription of the GFP reporter and the viral capsid protein VP39 were similar, indicating that there were no discernable differences in progression of the infection. Similarly, the production of GFP protein from the viral late gene promoter p6.9 and progeny virus appeared unimpaired (Figure 1B & C). Interestingly, qPCR (Figure 1A) and western blot data (Figure S1) indicated that expression of Cas9 and dCas9 were downregulated early in the infection cycle and was undetectable on western blot by 48 hpi.

Evaluation of CRISPR-mediated repression and disruption on GFP production

Initial experiments sought to establish transcriptional repression of the rBEV-encoded *gfp* gene infecting Sf9-dCas9 cells. Individual rBEVs with sgRNAs targeting the template (GFP1 and GFP4) and nontemplate (GFP2 and GFP3) strands within the *gfp* ORF were constructed, and repression of *gfp* transcribed with im-

mediate early (OpIE2), late (p6.9) and very late (p10) promoters was assessed. rBEVs encoding nontemplate strand-targeting sgRNAs showed a marked decrease in the proportion of GFP-positive cells and fluorescence intensity compared to the control at 48 hpi for OpIE2-GFP (Figure S2A). For p6.9-GFP and p10-GFP, there appeared to be a slight (p6.9-GFP) or significant (p10-GFP) reduction in GFP-positive cells compared to the control at 24 hpi, however there was no difference at 48 and 72 hpi (Figure 2A & S2B). Nevertheless, the fluorescence intensity for GFP2 and GFP3 targets was reduced compared to the control at all time points for p6.9-GFP, and 48 and 72 hpi for p10-GFP. Fluorescence intensity of rBEVs encoding strand targeting sgRNAs (GFP1 and GFP4) was indistinguishable from the control in all experiments, however, indicating potential strand bias for CRISPRi.

For CRISPRd experiments, p6.9-GFP rBEVs encoding sgRNAs GFP2, GFP3, and GFP4 were used to infect Sf9-Cas9 cells. For all 3 sgRNAs, the proportion of GFP-positive cells was significantly reduced compared to the control at all time points. The GFP2 sgRNA resulted in the lowest GFP-positive phenotype compared to GFP3 and GFP4. Significantly, whereas the proportion of GFP-positive cells was higher at 24 hpi and increased by 48 hpi for GFP3 and GFP4, the rBEV encoding the GFP2 sgRNA was less than 10% GFP-positive at 24 hpi and did not increase as the infection progressed. For the fluorescence intensity measurements of the GFP-positive cells, though, the GFP2 sgRNA rBEV was only slightly reduced compared to the untargeted control rBEV. Conversely, the GFP3 and GFP4 sgRNAs had significantly reduced fluorescence intensity compared to both GFP2 and control (Figure 2C & D).

Importantly, parental Sf9 cells infected with each of the p10-GFP (data not shown) and p6.9-GFP rBEVs produced fluorescence intensity measurements that were both increased compared to the same infections in either Sf9-Cas9 or Sf9-dCas9 cells, and were also all similar to the control (i.e. untargeted) rBEV. Finally, release of progeny BV was not statistically different for any of the viruses replicating in any cell line (Figure S3). Taken together, these data indicate that production of GFP was influenced by the presence of both (d)Cas9 and sgRNA and was unaffected in the absence of either of these molecules.

Extension of CRISPRi and CRISPRd to endogenous AcMNPV ie-1 and vlf-1

Next, the ability of the CRISPRi and CRISPRd systems to affect the production of endogenous AcMNPV genes was assessed (Figure 3). Spacer sequences were selected to target the *ie-1* and *vlf-1* genes encoding immediate-early protein 1 (IE-1) and very late factor 1 (VLF-1), respectively. The *ie-1* gene encodes a transcriptional activator, and is essential for viral DNA replication, late gene expression, and subsequent progeny virus production. The *vlf-1*gene encodes a transcriptional activator for the very late class of genes but has no effect on late gene promoters. Production of progeny virus and GFP transcribed from the p10 promoter was measured to assess the phenotypic impact of these targets in Sf9-dCas9 cells. Similar to previous experiments, the proportion of GFP-positive cells was reduced at 24 hpi for the IE1 sgRNA, however it increased by 48 hpi and was indistinguishable from the control. The proportion of GFP-positive cells was not affected for either IE2, VL1, or VL2. Reduced fluorescence for the rBEVs encoding nontemplate-targeting sgRNAs (IE1 and VL1), but not the sgRNAs targeting the template strand (IE2 and VL2) was observed. Finally, analysis of progeny virus production showed that the IE1 sgRNA reduced the infectious virus titer (IVT) ˜90% compared to the control at 48 hpi. The difference in IVT for the other targets was not statistically significant (Figure 3A).

For CRISPRd in Sf9-Cas9 cells, a marked reduction in GFP-positive cells was observed for both IE1 and IE2 sgRNA rBEVs, but not VL1 or VL2, at all time points. Fluorescence intensity was also significantly reduced for each sgRNA compared to the untargeted control. Since VLF-1 stimulates transcription from very late promoters but has no effect on late genes, rBEVs encoding the VL1 and VL2 sgRNAs and the p6.9-GFP expression cassette were prepared and used to infect Sf9-Cas9 cells. Importantly, analysis of fluorescence indicated no difference compared to the control rBEV for both VL1 and VL2 (data not shown). Finally, the IVT was reduced by ˜99% compared to the control for IE1 and IE2, and ˜64% for VL2. The measured IVT for VL1 was not statistically different from the control (Figure 3B).

Parental Sf9 cells infected with each of *ie-1* and*vlf-1* -targeted sgRNAs showed fluorescence and IVT levels

that were consistent with control (i.e. non-disrupted/repressed) levels, indicating that both (d)Cas9 and sgRNA are required for disruption or downregulation of *ie-1* and *vlf-1* (Figure 3C).

CRISPRd is more effective than CRISPRi for obstructing progeny BV release

Finally, rBEVs with sgRNAs targeting the *vp80* gene were prepared and evaluated for transcriptional repression and gene disruption. The*vp80* gene encodes the capsid-associated protein VP80, and its disruption prevents capsid assembly but has no effect on late gene expression. Fluorescence intensity of GFP transcribed from the late p6.9 promoter and progeny virus production were used to assess the effectiveness of CRISPRi and CRISPRd, and 4 sgRNAs were tested for CRISPRi and 2 for CRISPRd. The fluorescence intensity was similar for each *vp80* -targeting rBEV compared to the untargeted control in each cell line, and showed no differences when used to infect either Sf9, Sf9-Cas9, or Sf9-dCas9 cells (Figure 4A). Similarly, the IVT of infected Sf9 cell culture supernatants for each rBEV was similar, indicating unimpaired BV release in the absence of Cas9 or dCas9. The nontemplate strand-targeting VP2, VP3, and VP4 rBEVs reduced IVT ˜79%, ˜68%, and ˜57% compared to the control rBEV, respectively, in Sf9-dCas9 cells, while VP1 was similar to the control and to the IVT yielded from its infection to parental Sf9 cells. Infection with VP1 to Sf9-Cas9 cells, on the other hand, reduced the IVT by ˜98% compared to the untargeted control, and VP2 by ˜96% (Figure 4C). The latter result represents an ˜85% improvement over the result in Sf9-dCas9 cells. Finally, flow cytometry analysis indicated a reduction in total number of particles in culture supernatant for VP80 targets as compared to non-targeted control experiments in Sf9-Cas9 cells (Figure 4B).

Discussion

Recently, gene disruption based on CRISPR-Cas9 technology was reported in Sf9 and High Five cells, enabling the development of Sf9 cells with altered protein glycosylation capabilities . This technology was also applied to edit the AcMNPV genome for both gene disruption and knock-in, in which heterologous DNA was introduced to the AcMNPV genome in a site-specific manner . In that study, the editing efficiency was low for many of the targets tested despite previous reports of delivery of the required Cas9 and sgRNA components via ribonucleoprotein (RNP) complex as being more efficient than plasmid DNA in many cell lines . Although rBEVs with the desired mutation could be isolated through plaque purification, this strategy is not ideal for scrutinizing the effect of gene disruptions as it likely lacks the resolution necessary to determine the impact of the disruption on viral gene expression or replication without further processing steps such as plaque isolation and extensive screening.

The present study sought to develop an efficient and robust technology for targeted genome engineering that would be capable of scrutinizing the effect of gene disruption or repression on viral gene expression and replication. To this end, stable, transgenic Sf9 cell lines constitutively expressing the *cas9* or *dcas9* gene were developed. To test the efficacy of gene disruption and transcriptional repression using this approach, Sf9-Cas9 and Sf9-dCas9 cells were infected with rBEVs encoding both the sgRNA and the genetic target for disruption or repression. This strategy would ensure that every cell would receive the genetic code required for (d)Cas9 and sgRNA expression and thus present the highest probability for having the necessary resolution in the assay to observe the effects of the target gene disruption or repression.

Since downregulation of host protein expression due to infection with AcMNPV is a characteristic of the BEVS , experiments to assess expression of (d)Cas9 using qPCR and western blot were conducted. Consistent with prior studies, downregulation of dCas9 and Cas9 in the early stages of infection was observed. As this could impact the effectiveness of CRISPRi, the repression of *gfp* transcribed from immediate-early (OpIE2), late (p6.9) and very late (p10) promoters was evaluated to establish the efficiency of repression for promoters differing in temporal and relative strength expression characteristics. Significant reduction in fluorescence intensity was observed for each promoter, consistent with robust transcriptional repression mediated by CRISPRi. Additionally, the possibility of a 'strand bias' was observed in the BEVS system, in which robust transcriptional repression can only be achieved by targeting the sgRNA/dCas9 complex to the nontemplate strand. This phenomenon has been observed in various other prokaryotic and eukaryotic systems previously . Experiments conducted with Sf9-Cas9 cells (CRISPRd) showed decreased fluorescence

intensity measurements compared to the control, and contrary to CRISPRi where the proportion of GFP-positive cells was not affected, the population of GFP-positive cells was significantly reduced. Notably, the GFP2 target reduced the GFP-positive cell population to less than 5%. Despite this, fluorescence intensity was higher in GFP-positive Sf9-Cas9 cells than infections in Sf9-dCas9 cells with the same rBEV. This observation is presumably due to the mechanisms by which CRISPRd and CRISPRi function; for CRISPRi, successful targeting blocks transcript elongation and leads to a reduction in mRNA produced and translated by the cell. This ultimately leads to an overall reduction in fluorescence intensity. Gene disruption mediated by CRISPRd results in indel mutations from dsDNA break repair, and protein expression is impacted by translation but not transcription . Any gene copies that are not successfully targeted or the indel mutation is silent would be transcribed and translated at wild-type levels.

Finally, endogenous AcMNPV *ie-1* , *vlf-1* and *vp80*genes were targeted for transcriptional repression and gene disruption. The IE-1 protein is the major transcriptional regulator of AcMNPV and is responsible for *trans* -activation of several known early genes. Importantly, it is one of several genes required for late gene expression and viral genome replication . Deletion of the *ie-1*gene results in loss of infectivity . The VLF-1 protein is a regulator of very late gene transcription and is responsible for the 'transcriptional burst' observed for the very late class of genes; purified VLF-1 stimulated transcription of the very late polh promoter in a concentration depended fashion but had no apparent effect on the late 39k promoter . Complete deletion of the *vlf-1* gene may also impair assembly of BVs, although DNA replication and late gene transcription appeared to be reduced but permitted . On the other hand, the *vp80* gene encodes a capsid-associated protein that is essential for BV production but is not essential for viral late gene expression . Selection of these endogenous genes provided the ability to observe the efficacy of CRISPRi and CRISPRd in several ways; repression/disruption of *ie-1* should impact the entire infection cycle of the rBEV, while targeting *vlf-1* should reduce expression from the very late p10 promoter but not the p6.9 promoter. Finally, disruption of *vp80* expression should impact the production of progeny BV but not inhibit late gene expression.

Indeed, infections with rBEVs encoding sgRNAs targeting each of these genes yielded the expected result in all three cases; significant reduction in both GFP and progeny virus production for IE-1 targets, reduced BV production but unimpaired late gene expression for VP80 targets, and targeting VLF-1 led to a reduction in fluorescence intensity for GFP expressed from the p10 promoter but not p6.9. Interestingly, although there appears to be a reduced IVT for VL1 and VL2 rBEVs in Sf9-Cas9 cells (˜42% and ˜64%, respectively) and for VL1 in Sf9-dCas9 cells (˜50%) , only the VL2 rBEV IVT was statistically different from the control. This could indicate that either the resolution in the assay is not sensitive enough to detect this difference or that enough VLF-1 was produced to permit replication and production of progeny virus to near-wildtype levels. Nevertheless, these results agree with a previous study in which deletion of the*vlf-1* gene had no effect on late gene transcription but substantially reduced expression from the very late p10 promoter . Unsurprisingly, the template-targeting sgRNA VP1 did not result in reduced progeny virus production in Sf9-dCas9 cells. Targeting the*vp80* gene with nontemplate-targeting sgRNAs VP2, VP3, and VP4, however, reduced IVT by ˜79%, ˜68%, and ˜57%, respectively, in this cell line. Similar to VLF-1 targets, though, the reduction in IVT with the VP4 sgRNA was not statistically significant. Given that transcriptional repression efficiency has been observed to be inversely correlated to the distance of the target spacer sequence from the transcriptional start site , it may not be entirely surprising that this sgRNA was less effective.

In addition to the apparent strand bias in the experiments with Sf9-dCas9 cells, the proportion of cells displaying a GFP-positive phenotype at 24 hpi was substantially lower for the IE1 rBEV as compared to the other infections, while fluorescence was substantially reduced at all time points and for both targets in Sf9-Cas9 cells. Analysis of the replication of rBEVs through EPDA on culture supernatants at 48 hpi also showed ˜90% decrease in the rBEV titer for IE1 compared to controls for CRISPRi and ˜99% for CRISPRd. This latter result is significant since a report in which transformed Sf9 cells expressing a ˜470 bp dsRNA molecule targeting the AcMNPV *ie-1* gene exhibited strong viral repression at early stages of infection but subsequent recovery of viral proliferation was observed by the late stages of the infection cycle .

Deletion of the *vp80* gene has previously been shown to prevent BV production whilst permitting replication

of viral DNA and transcription of viral late genes at or near wild-type levels. Results presented here support these conclusions: production of GFP was similar for each virus in Sf9-dCas9, Sf9-Cas9, and the parental Sf9 cells, however production of progeny virus was decreased by >90% in Sf9-Cas9 cells. Interestingly, the supernatant from Sf9 cells infected with the Δ*vp80* -rBEV in that study appeared to have undetectable IVT . Assessment of infected culture supernatants at 4, 8, and 12 hpi here and previously , however, revealed IVT ˜10^4 -10^5 pfu/ml at each time point (data not shown). This could indicate incomplete viral uptake in the early stages of infection before the onset of progeny BV release. Further, the *trans-* complementation strategy resulted in a ˜25-fold decrease in BV seed production and constitutive expression of the *vp80* gene appeared unstable or toxic to Sf9 cells. Finally, higher MOI (MOI = 10) was required in order to produce recombinant protein at the same level as the wild-type rBEV . In this study, there was no difference in GFP production at MOI = 3 and each of the rBEVs displayed no indication of impaired replication in Sf9 cells. Taken together, this strategy may contribute to reduced downstream processing complexity by minimizing rBEV contamination. Nevertheless, targeted disruption of *vp80* reduced the IVT by ˜98% and ˜96% for VP1 and VP2, respectively. Compared to CRISPRi, these results indicate that CRISPRd may be more effective for reducing progeny virus production. Finally, to ensure that targeting *vp80* resulted in a reduction of particles released to the culture supernatant as opposed to the release of defective particles that are not infectious, flow cytometry was used to analyze supernatants from several control and VP80-targeted infections in Sf9-Cas9 cells. Indeed, the results indicate ˜90% reduction in particle concentration in the VP80-disrupted infections as compared to the control. Consistent with previous reports in which the ratio of total particles quantified using flow cytometry to IVT measured using EPDA ranged from 1 to 10 , the FC:IVT ratio in the samples analyzed was ˜5-10 as well.

Concluding remarks

Taken together, the phenotypes observed in this report are consistent with disruption or repression of the endogenous AcMNPV *ie-1* ,*vlf-1* , *vp80* genes. The results indicate that CRISPRd may be more effective than CRISPRi for total disruption of target genes, whereas CRISPRi allows expression of the targeted gene at levels that are lower than the wildtype, suggesting it may be more appropriate for targets that are not amenable to deletion. Consequently, the CRISPRd tool developed here may be more useful for evaluating the essentiality of endogenous AcMNPV genes and reducing BV contamination in culture supernatants, whereas CRISPRi may be more effective for use in prolonging the infection cycle and accompanying bioprocess in order to increase yield of the target recombinant molecule. This report serves as a foundation for further improvement of the BEVS as a platform for recombinant protein therapeutics.

Conflicts of Interest

The authors declare no conflicts of interest.

Acknowledgements

This work was supported in the form of a Natural Sciences and Engineering Research Council of Canada (NSERC) post-graduate scholarship to M.R.B, and NSERC Discovery (RGPIN 355513-2017) and Strategic Project Grants (STPGP 462995-14) to M.G.A. We thank D. Theilmann for kindly donating the plasmid pOpIE2E2.3 and Dr. Aaron P Frenette for help with western blotting.

References

Tables

Table 1. Protospacer sequences for sgRNA targets.

rBEV	Target	Protospacer Sequence (5'-3')	PAM	Strand
Control	n/a	caccttgaagcgcatgaact	n/a	n/a
GFP1	gfp	gggcaagggcaacccctacg	agg	Template
GFP2	gfp	gtcgtaggcgaagggcaggg	ggg	Nontemplate

rBEV	Target	Protospacer Sequence (5'-3')	PAM	Strand
GFP3	gfp	gttgccgtactggaacacgg	tgg	Nontemplate
GFP4	gfp	ccgagggctaccactgggag	agg	Template
IE1	ie-1	accgtgtcggctccatccgggg	tgg	Nontemplate
IE2	ie-1	tgatatctgacagcgagactg	cgg	Template
VL1	vlf-1	acacggactcgaaccggggag	cgg	Nontemplate
VL2	vlf-1	ggcaacgatgcacgcccgacg	agg	Template
VP1	vp80	gcccgccgcaatcgccgccg	cgg	Template
VP2	vp80	gctggatgttacccgcgg	cgg	Nontemplate
VP3	vp80	tcgatgcggccaggtcgc	tgg	Nontemplate
VP4	vp80	gcggatcgctaaatgccg	tgg	Nontemplate

Figure Captions

Figure 1. Sf9-Cas9 and Sf9-dCas9 cells are indistinguishable from the parental Sf9 cell line. A. QPCR expression analysis of virus-encoded *vp39* and *gfp* reporter gene are not affected by the presence of either *cas9* or *dcas9*expression. Both *cas9* and *dcas9* are downregulated in response to infection. **B.** GFP fluorescence intensity and**C.** progeny virus production are similar between all cell lines.

Figure 2. CRISPR-mediated targeting of GFP transcribed from the late p6.9 promoter. Percentage of population that is GFP-positive and fluorescence intensity of *gfp* - targeting rBEVS in Sf9-dCas9 cells (**A.** and **B.**), and Sf9-Cas9 cells (**C.** and**D.**), respectively.

Figure 3. CRISPR-mediated targeting of the AcMNPV *ie-1*and *vlf-1* genes. Percent GFP-positive, fluorescence intensity, and IVT for rBEVs in **A.** Sf-dCas9, **B.** Sf9-Cas9, and**C.** parental Sf9 cells.

Figure 4. CRISPR-mediated targeting of the AcMNPV *vp80*gene. A. Mean fluroescent intensity for *vp80* -targeting and control rBEVs in Sf9-Cas9, Sf9-dCas9, and parental Sf9 cells.**B.** Total particles in culture supernatants of infected Sf9-Cas9 cells and **C.** IVT for control and *vp80* -targeting rBEVs in each cell line at 48 hpi.

Figure 1

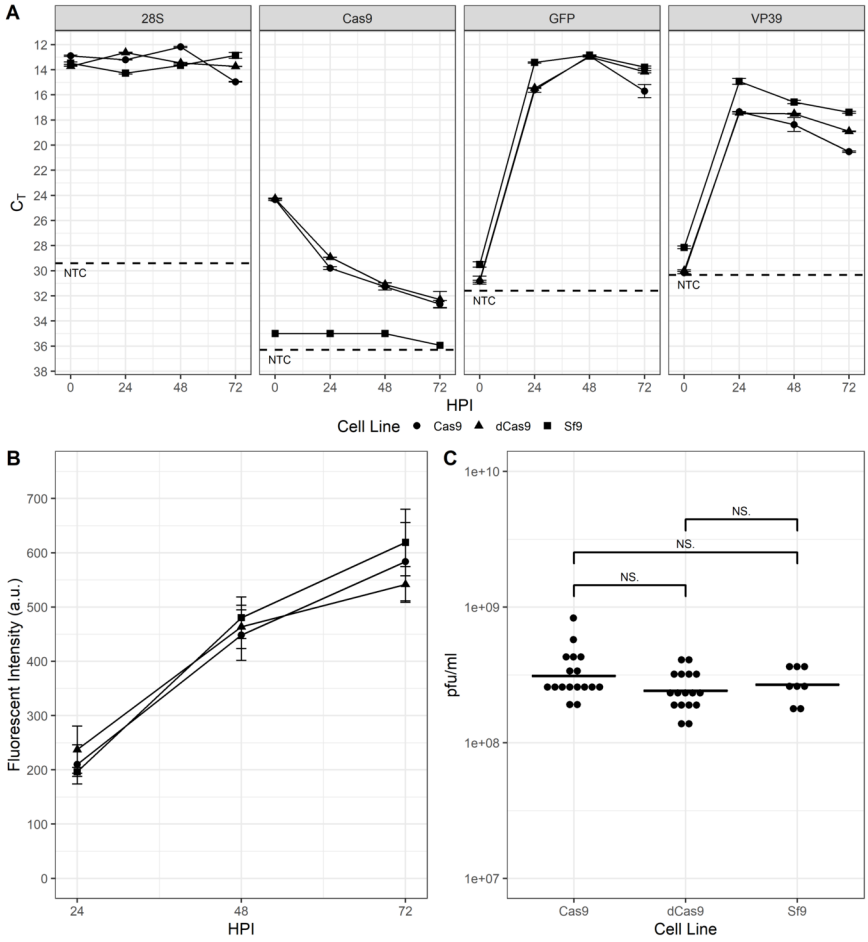

Figure 2

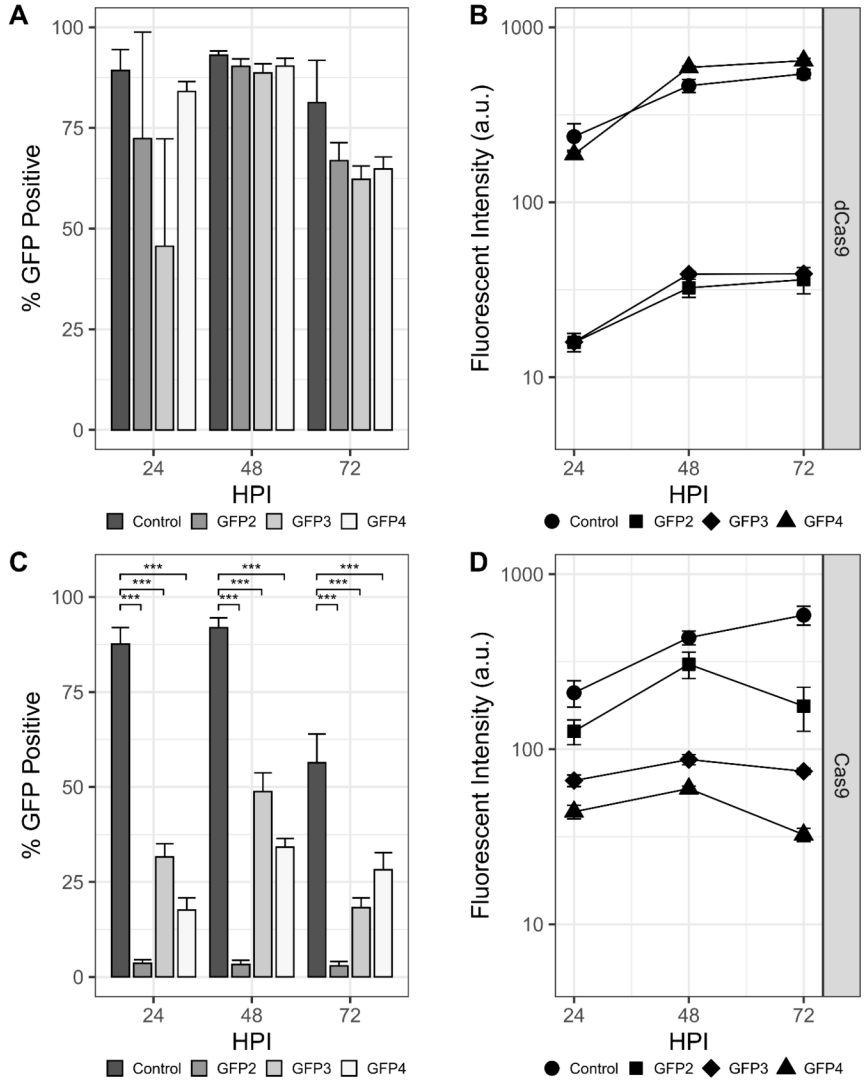

Figure 3

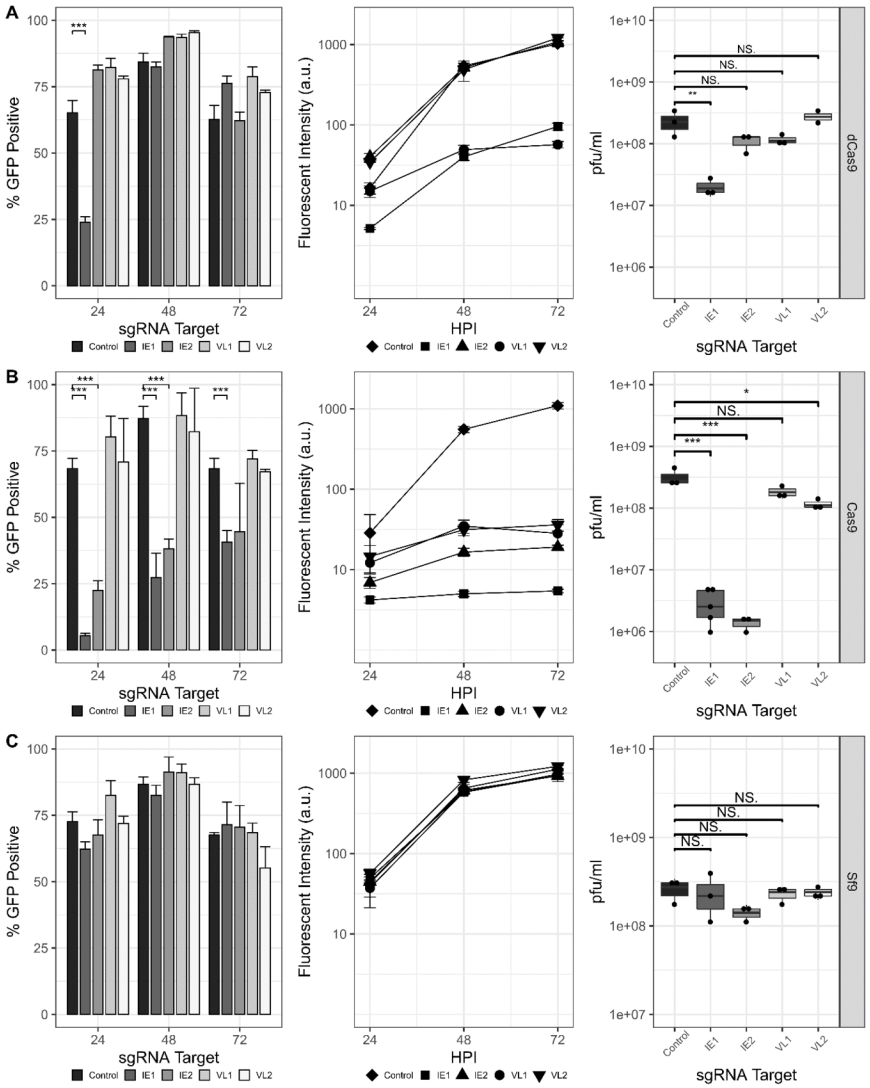

Figure 4